Comparative Performance of Steel Drainage Pipes against Flood-induced Deformation in River Levee

Jenisha Singh[1], Kazuki Horikoshi[2], Yusuke Mochida[3] & Akihiro Takahashi[4, *]

[1] School of Civil Engineering, Central South University, Changsha, China / Formerly, Department of Civil and Environmental Engineering, Tokyo Institute of Technology, Tokyo, Japan

[2] Assistant Professor, Department of Civil and Environmental Engineering, Tokyo Institute of Technology, Tokyo, Japan

[3] Nippon Steel Corporation Research & Development, Futtsu, Japan

[4] Professor, Department of Civil and Environmental Engineering, Tokyo Institute of Technology, Tokyo, Japan

[*] Corresponding author (takahashi.a.al@m.titech.ac.jp)

Geotechnical and Geological Engineering, 40(9), 4847-4857, 2022

Original URL:

https://doi.org/10.1007/s10706-022-02166-x

Abstract

Steel drainage pipes that can provide both drainage and reinforcement functions are expected to give better performance in levee protection against flooding compared to the protection that can provide only either one of these functions. This study investigates the effectiveness of steel drainage pipes that combine the drainage and reinforcement functions against flooding in comparison with the pipes having only either drainage or reinforcement function through the finite element analysis validated by the simulation of the centrifuge model tests. The analysis results reveal that drainage function is crucial in minimisation of deformation, while the use of steel drainage pipe protection is more reliable as protection is available in form of reinforcement even when drainage function has deteriorated. Levee protected only with reinforcement and only drainage pipes experienced 112% and 2.4% larger settlements respectively in comparison to levees protected with steel drainage pipes. The performance of a levee reinforced by steel drainage pipe against flooding is more redundant and reliable compared to the traditional method of protection which provides only one of the functions.

Keywords: levee; seepage; finite element analysis; steel drainage pipes

1 Introduction

River levees during the flooding event in the absence of the proper protection sometimes experience a large deformation, and in the worst-case scenario, even the breaching of the levee is observed. Deformation is the result of the reduction of matric suction due to saturation of the levee caused due to increased seepage flow during the flood (Hamdhan and Schweiger, 2011; Polemio and Lollino, 2011; Vandamme and Zou, 2013). Traditionally, there are two different approaches to designing the protection measures in the levee. The first method of protection is providing additional strength through reinforcement, (Rotte and Viswanadham, 2012; Yang and Deng, 2019; Zhou et al., 2009) and another method is minimising the strength reduction through drainage (Rahardjo et al., 2003, 2011; Saran and Viswanadham, 2018). In this study use of steel drainage pipe which combines both traditional approaches of protection by providing drainage and reinforcement is proposed.

Steel drainage pipes are tubular steel pipes with numerous holes on the surface and also have spiral blades at the end. Steel drainage pipes because of their tubular structures, surface holes, and spiral blades can provide both reinforcement and drainage functions. A Series of centrifuge experiments were performed by Singh et al. (2019) to understand the working mechanism of these steel drainage pipes. Unfortunately, as the same flood pattern could not be given to all the models, the relative performance of the steel drainage pipe could not be confirmed. In this paper, through finite element modelling, a comparative study of steel drainage performance against its traditional counterpart with only either drainage or reinforcement function is made under the same flooding condition.

A Series of the six different cases of the centrifugal tests were performed at the centrifugal acceleration of 20g by Singh et al. (2019). Centrifuge experiments were performed for its better capillary condition and realistic stress condition in the physical model ground. For all the test cases, a half section of the river levee made of Edosaki sand with a side slope of 1H: 1V was modelled. Six different cases of varying levels of protection were investigated during the study. In the centrifuge study since the same level of flooding was not achieved, direct comparison to study performance was rather difficult. For this purpose, a numerical simulation of four different cases of unreinforced levee case, the levee with proposed steel drainage pipes, the case with only reinforcement pipes and the case with drainage pipes is presented in this study. Four of the cases and their test conditions are summarised in **Table 1**. **Figure 1** shows the geometry of the model slope and arrangement of pipes in the centrifuge models. Here and after all the dimensions are in the prototype scale. In Cases 3, 4, and 6, pipes are installed at a 1m height from the toe of the slope. The model consisted of three sections; the water supply section, the model ground section, and the drainage section collecting drained seepage water. In Cases 3, 4, and 6, three pipes were installed at a horizontal spacing of 1 m and an elevation of 1 m from the ground surface. In Cases 3 and 4, steel pipes were used, whereas in Case 6, pipes made of flexible perforated Silicone pipes were used. In all the cases, the surface layer of 0.2 m made of soil mixed with fibre was provided.

During the test, the foundation layer was first saturated in 1g condition, and the flood was simulated by raising the water level in the supply section in 20g condition. In Cases 1, 3 and 4, the rising rate of the flood water was small and was in a range of 0.03-0.06 m/hr, while that was large and was around 0.3 m/hr in Case 6. If the topographical conditions in Japan are taken into consideration, the rising rate of flood water level 0.03-0.06 m/hr is rather slow while the rising rate of 0.3m/hr is a reasonable value. This difference in the rising rate did not allow direct comparison on time reference among all the cases. Experiment results showed that steel drainage pipes through the drainage function limited rise of the phreatic surface, and the rigid pipe provided additional reinforcement against flooding. From the experiment, while the working mechanism of steel drainage was confirmed, the comparative performance of steel drainage pipe with its counterpart having only one of the functions of drainage or reinforcement could not be confirmed explicitly.

2 Numerical analysis method validation

2.1 Constitutive models used

Three-dimensional finite element analysis is conducted using the finite element code developed by the last author. First validation is made by comparative studies of the numerical analysis and centrifuge experiment results having different flooding patterns. Equations solved in the numerical analysis are described here.

The equilibrium equation for soil is expressed as

$$\frac{\partial \sigma_{ji}}{\partial x_j} + \bar{\rho} b_i = 0 \tag{1}$$

where density with soil, water and air mixture $\bar{\rho}$ is given by

$$\bar{\rho} \equiv n S_r \rho_w + (1-n)\rho_s \tag{2}$$

Here, σ_{ij}= total stress, ρ_w= density of water, ρ_s = soil particle density, n = porosity, S_r = degree of saturation.

Governing equation for pore water is expressed as

$$S_r \dot{\varepsilon}_{jj} + C\dot{h}_p + \frac{\partial}{\partial x_i}\left(-k_{wu}\frac{\partial h}{\partial x_i}\right) = 0 \tag{3}$$

In Equation (3), C is referred to as specific moisture capacity from the soil-water characteristic curve (corresponds to the slope of the relationship between pressure head with volumetric water content). In the equation, h and h_p represent the total head and pressure head ($= \frac{u_w}{\rho_w g}$), respectively. Pore air pressure (u_a) is assumed to be equal to atmospheric pressure which is a reasonable assumption as the monotonic rise of a phreatic surface due to flooding is considered in this study. k_{wu} is unsaturated hydraulic conductivity. Unsaturated hydraulic conductivity is calculated from specific permeability k_{wr} (ratio of unsaturated hydraulic conductivity k_{wu} to saturated hydraulic conductivity, k_{ws}) and the model proposed by Kosugi (1999) is used;

$$k_{wr} = S_e^{0.5}\left\{1 - \left(1 - S_e^{1/m}\right)^m\right\}^2 \tag{4}$$

where S_e = effective degree of saturation. In the computation, the soil is modelled as an elastoplastic material and the Drucker-Prager model (Drucker and Prager, 1952) is used for the yield surface and the effective stress σ'_{ij} is expressed using equation proposed by Bishop (1960);

$$\sigma_{ij}' = \left(\sigma_{ij} - u_a\right) + \chi(u_a - u_w) \tag{5}$$

with $\chi = S_e$. van Genuchten model (van Genuchten, 1980) is used for modelling the soil-water characteristic curve (SWCC) of the unsaturated soil. Using the van Genuchten closed-form equation, S_e. is calculated as the function of the suction.

2.2 Numerical analysis conditions

2.2.1 Modelling of the river levee

River levees in the analysis are modelled as in the centrifuge experiment. The properties of the soil used in numerical analysis are presented in **Table 2**. The foundation bottom is modelled as an impermeable layer and fixed rigid connection (displacement is constrained to zero). The sides of the foundation on the protected side are modelled as impervious surfaces. As for the displacement constraint, vertical side boundaries are constrained in the horizontal direction. All the other boundary is considered permeable and there is no constraint in displacement. The boundary condition and the geometry with mesh used in the analysis are summarised in **Fig. 2**. Eight node brick elements are used in modelling both solid and liquid phases. For the solid phase, the B-bar method is employed to avoid volumetric locking. The uniform size of the mesh is used in the analysis as far as possible. In the mesh, the number of nodes and elements are 3393 and 2688 respectively.

2.2.2 Modelling of pipes

The proposed steel drainage pipe is 6 meters long, with two different sections. These two sections are; 1m long section having the spiral ring made of 1 cm thick metal plate having a pitch of 16 cm at the end and a 5-meter long section without spiral rings. For the numerical analysis, the spiral ring is not considered and only the embedment length of the pipe in the centrifuge experiment which is 5.6 m is considered and placed at a horizontal spacing of 1 m and an elevation of 1 m from the ground surface. The dimension and properties of the steel drainage pipe used in the analysis are listed in **Table 3**. The drainage function is modelled as the line of the nodes with a pressure head ceiling at the elevation of the nodes indicating the free flow inside the pipes. The reinforcement function in the slope is modelled by adding the series of elastic beam elements at the location of the pipe. Nodes for the beam element are common to the nodes of the elements that model soil. So no slip between the pipe and soil is considered. The relative movement is considered by the shear deformation of adjacent soil elements. Pipes with only either of the functions are also modelled using drainage or reinforcement function only.

2.2.3 Flood simulation

Flooding conditions are kept similar to the experiment condition. Each analysis is divided into two phases. In the first step, a steady state before flooding is achieved by assigning the water level at the foundation ground surface. This result is used as the initial condition for the second step. The flooding is simulated in the second step of the analysis, which is a transient analysis. In this step, the flood is simulated by increasing the water level on the right side of the model. **Figure 3** shows the time histories of the supply flood water head for the centrifuge experiment. In the numerical analysis for validation, the flooding is modelled as a step-wise change of the flood water head in the experiment. Each step is kept five hours long and in each step, the flood head is kept constant. The flood head at each step is kept the same as in the centrifuge experiment at the end of each period. **Figure 3** also shows the flood used for the numerical analysis later with the same flooding condition.

2.3 Numerical analysis result comparison with centrifuge result

Before making the comparisons under the same flooding condition, the numerical analysis method is validated with the comparison with the centrifuge results. The flood water head used in the centrifuge experiment (not Num_Flood in **Fig. 3**) is applied in this series of analyses. **Figure 4** shows the comparisons of the time histories of pore water pressure recorded at Locations A and B (see **Fig. 1**) in the experiment and numerical analysis for Cases 1, 3, 4 and 6. In the figure, it can be observed that the trend of rising and falling of pore water pressure with increase and decrease flood head is captured by the numerical analysis. The parameters here are adjusted such that the temporal change is matched in the numerical analysis. The magnitude is not exactly the same as the experiment result; however, from the results, it can be observed that the effect of drainage and the consequent change in pore water pressure is simulated by numerical analysis.

Figure 5 shows the comparisons of the axial force observed near the slope (0.4m away from slope surface) in the experiment and numerical analysis along with the flood head used in numerical analysis in Cases 3 and 4, respectively. Axial force here in both experiment and numerical analysis is shown by considering the axial force at the start of the seepage flow as zero. Thus, the axial force can be negative during an increase and decrease of the tensile force. The axial force simulated in both cases is similar in the trend and magnitude. The change in the axial force with the seepage flow is well captured by numerical analysis in both cases when drainage is present (Case 3) and when drainage is not present (Case 4).

Figure 6 shows the comparison of the time histories of settlement at Location F for Cases 1 and 6. From the figure, it can be observed that the trend of the increase of settlement and also the point of initiation of failure indicated by the sharp change in the value of the settlement is well captured by the numerical analysis. Since the experiment allowed the installation of a limited number of sensors, the comparison is made with the settlement of the slope only. The displacement is not very comparable, but the timing of the slope failure is predicted which is relevant in a comparative study of protection in a levee. In Cases 3 and 4, as minor local erosion was observed in the experiment and this cannot be modelled in the present numerical analysis, no comparison of displacement is shown for these cases. However, since the calculated axial force of the pipe is comparable to the experiment as shown in **Fig. 5**, it can be said that the deformation of the slope can be reasonably captured in these cases.

Overall, the numerical analysis method used in the study can reasonably simulate the flood-induced seepage in the river levee and also the effect of the drainage and reinforcement. Hence, this numerical analysis method is used in the simulation with the same flooding condition.

3 Comparative study of different protection measures against flood-induced deformation

For the comparative performance of the steel drainage pipe with the protection measures having only one of the functions of drainage or reinforcement, a three-dimensional finite element numerical analysis is performed with the same flooding condition using the same river levee model in the centrifuge experiment and numerical validation. In the analysis, four different Cases A.1, A.3, A.4, and A.6 are taken into consideration. In these four cases, a different level of protection is provided, which is tabulated in **Table 1**. For the flood simulation, the model flood hydrograph similar to the rising rate in the centrifuge test in Case 6 (Num_Flood in **Fig. 3**) is used for all the cases in this series of analyses. The flood head in the numerical simulation is increased in a stepwise manner in three steps of 2.5 hours long and kept constant at the maximum level for the levee for all the cases of consideration.

Figure 7 shows the time histories of the settlement at the shoulder of the slope and horizontal displacement at the toe of the slope, respectively, for all the cases. It can be observed that with the use of protection in the river levee, the displacement is reduced significantly. In the cases where the drainage is provided (Cases A.3 and A.6) both horizontal displacement and settlement are reduced significantly, highlighting the importance of the drainage function in the protection. In Case A.4 (only reinforcement), the rate of displacement increase is similar to Case A.1 (unreinforced) in the initial stage (0-15 hrs), while further increase in the displacement is restrained after that. Maximum settlement and horizontal displacement in Case A.4 are almost three times those in Case A.3 (steel drainage pipes). With the use of the only drainage (Case A.6) the settlement in the model ground is minimised to the same extent as in the use of the steel drainage pipe (Case A.3). This implies that the reinforcement function is not fully utilised in Case A.3 in the scenario considered in the analysis. However, with the use of the steel drainage pipe, reinforcement may act as the backup protection in the scenario when the drainage function is deteriorated possibly by blockage of pipes. In the study of the use of drainage pipes made of geosynthetic material by Ozer and Akay (2021); and Saran and Viswanadham (2018), it was observed that clogging drainage pipes greatly affected the performance of sand slopes. Thus composite geosynthetic pipes with the dual function of drainage and reinforcement were proposed for better protection in the study by Ozer and Akay (2021). The steel drainage pipes provide redundant and more reliable protection to the river levee. The observation and consideration above indicate that Case A.3 (steel drainage pipe) can provide the best protection among the cases.

Figure 8 shows the location of the phreatic surfaces after 40 hours of seepage flow for all the cases. Reasons for choosing the elapsed time of 40 hrs as a reference point are that at this point the supply flood level is at maximum level, and the change in displacement in most of the cases is stable. In the figure, it can be observed that with the presence of drainage, the location and shape of the phreatic surface in the levee are modified. The phreatic surface is at a lower position and has a concave upward shape in the cases with the drainage, whereas in the absence of the drainage, the shape is concave downward and the location is high. With reference to **Fig. 7**, it can be said that this limited rise in phreatic surface causes limited saturation of the river levee and thus ultimately limiting deformation in cases with drainage. Also, the presence of the reinforcement (Case A.4) ensures less deformation compared to Case A.1 (unreinforced) even though the level of the phreatic surface is similar in both cases. Table 4 summarises the performance of different cases in terms of the maximum settlement, maximum horizontal displacement and cross-sectional area of the levee in the unsaturated condition after 40 hrs of seepage flow. The table also indicates the percentage change of these parameters in comparison to Case A.3 (case with steel drainage pipes).

Figure 9 shows the axial force distribution in the pipe in Cases A.4 and A.3 (cases with only reinforcement and steel drainage pipes) at the different elapsed times of seepage flow (0, 10, 15, 20, 30 and 40 hrs). Here, the axial force shown here is the total value including the force induced by the self-weight of the soil before flooding. (As the plots in **Fig. 5** are the increment from the steady-state before flooding; a direct comparison cannot be made with this figure.) **Figure 10** shows the location of the phreatic surfaces at the elapsed time of 0, 10, 15, 20, 30, and 40 hrs of seepage flow for Case A.4 and Case A.3, respectively. With the elapsed time the phreatic surface moves above the location of the pipes in Case A.4, whereas there is not much change in position in Case A.3. This movement of the phreatic surface above the pipes causes larger axial force mobilisation in Case A.4. In Case A.3, since there is not much change in the location of the phreatic surface, axial force mobilised remains similar even after a longer duration of seepage flow. Mobilisation of large axial force in Case A.4 is responsible for limiting the deformation even after the rise in phreatic surface to a higher level in the river levee.

4 Conclusions

This study investigates the effectiveness of steel drainage pipes which combine the drainage and reinforcement function against flooding on a sand levee with a 1H:1V slope in comparison with the pipes having either drainage only or reinforcement function through the finite element analysis validated by the simulation of the centrifuge model tests. It is observed that drainage is crucial in minimising the horizontal displacement and settlement of the levee. Compared to the unreinforced case, the use of only reinforcement reduces the settlement and horizontal displacement in levees significantly by mobilisation of axial force, but the maximum horizontal displacement is 193% larger and maximum settlement is 112% larger compared to the use of steel drainage pipes. With the use of the only drainage, while the maximum settlement in the model ground is minimised to a similar extent (only 2.4% larger) as in the use of the steel drainage pipes, the maximum horizontal displacement is 37.2% larger compared to the use of steel drainage pipes. In addition, the use of steel drainage pipe protection is more reliable as protection is available in form of reinforcement even when drainage function has deteriorated. Thus, the performance of a levee reinforced by steel drainage pipes against flooding is more redundant and reliable compared to the traditional method of protection which provides only one of the functions when subjected to the same flooding. The slope considered in this study is an example of an extreme case, however, the performance of the purposed steel drainage pipes is also expected to be effective to prevent or minimise the possible failure in a gentler slope. While in this comparative study erosion of soil around the pipe is not taken into consideration, the relative performances may be influenced when the pipes are provided with drainage and erosion occurs. Ensuring that erosion of soil is limited especially near the surface would allow more reliable protection against flooding with the use of steel drainage pipes.

Data availability

The datasets generated during and/or analysed during the current study are available from the corresponding author on reasonable request.

Acknowledgements

The first author would like to gratefully acknowledge the support provided by the Monbukagakusho (Ministry of Education, Culture, Sports, Science, and Technology) scholarship for graduate students. The work presented in this paper is part of the collaborative research with the Nippon Steel Corporation.

References

Bishop, A., 1960. The measurement of pore pressure in the triaxial test, In: Pore Pressure and Suction in Soils. Butterworth & Company, London, Butterworth, London, pp. 38-46.

Drucker, D., Prager, W., 1952. Soil mechanics and plastic analysis or limit design. Quart. Appl. Math. 10, 157-175.

Fredlund, D., Rahardjo, H., Fredlund, M., 2012. Unsaturated soil mechanics in engineering practice. John Willey & Sons. Inc., Hoboken, New Jersey, USA.

Hamdhan, I.N., Schweiger, H.F., 2011. Slope Stability Analysis of Unsaturated Soil with Fully Coupled Flow-Deformation Analysis, In: Mathematical Geoscience at the Crossroads of Theory and Practice. Salzburg, Austria. DOI:10.5242/iamg.2011.0063

Kosugi, K., 1999. General model for unsaturated hydraulic conductivity for soils with lognormal pore-size distribution. Soil Sci. Soc. Am. J. 63, 270-277. DOI:10.2136/sssaj1999.03615995006300020003x

Ozer, A.T., Akay, O., 2021. Investigation of drainage function of geosynthetic for basal reinforce embankment. Int. J. Phys. Model. Geotech. 1–51. https://doi.org/10.1680/jphmg.21.00032

Polemio, M., Lollino, P., 2011. Failure of infrastructure embankments induced by flooding and seepage: a neglected source of hazard. Nat. Hazards Earth Syst. Sci 11, 3383-3396. DOI:10.5194/nhess-11-3383-2011

Rahardjo, H., Hritzuk, K.J., Leong, E.C., Rezaur, R.B., 2003. Effectiveness of horizontal drains for slope stability. Eng. Geol. 69, 295-308. DOI:10.1016/S0013-7952(02)00288-0

Rahardjo, H., Santoso, V.A., Leong, E.C., Ng, Y.S., Hua, C.J., 2011. Performance of Horizontal Drains in Residual Soil Slopes. Soils Found. 51, 437-447. DOI: 10.3208/sandf.51.437

Rotte, V.M., Viswanadham, B.V.S., 2012. Performance of 2V:1H Slopes with and without Soil-Nails Subjected to Seepage: Centrifuge Study, In: GeoCongress, ASCE. pp. 643-652.

Saran, R.K., Viswanadham, B.V.S., 2018. Centrifuge model tests on the use of geosynthetic layer as an internal drain in levees. Geotext. Geomembranes 46, 257-276. DOI:10.1016/j.geotexmem.2017.12.004

Singh, J., Horikoshi, K., Mochida, Y., Takahashi, A., 2019. Centrifugal Tests on Minimization of Flood-induced Deformation of Levees by Steel Drainage Pipes. Soils Found. 59, 367-379. DOI:10.1016/j.sandf.2018.12.008

van Genuchten, M., 1980. A closed-form equation for predicting the hydraulic conductivity of unsaturated soils. Soil Sci. Soc. Am. J. 44, 892-898. DOI: 10.2136/sssaj1980.03615995004400050002x

Vanapalli, S., Fredlund, D.G., Pufahl, M.D., Clifton, A.W., 1996. Model for the prediction of shear strength with respect to soil suction. Can. Geotech. J. 33, 379-392. DOI: 10.1139/t96-060

Vandamme, J., Zou, Q., 2013. Investigation of slope instability induced by seepage and erosion by a particle method. Comput. Geotech. 48, 9-20. DOI:10.1016/j.compgeo.2012.09.009

Yang, M., Deng, B., 2019. Stability study of slope reinforced with piles under steady unsaturated flow conditions. Comput. Geotech. 109, 89-98. DOI:10.1016/j.compgeo.2019.01.020

Zhou, Y.D., Cheuk, C.Y., Tham, L.G., 2009. Deformation and crack development of a nailed loose fill slope subjected to water infiltration. Landslides 6, 299-308. DOI:10.1007/s10346-009-0162-7

Table 1 Protection conditions in models

Case	Level of protection	Description of protection					
		Pipe 1		Pipe 2		Pipe 3	
		R	D	R	D	R	D
Case 1/A.1[c]	Unreinforced	N/A	N/A	N/A	N/A	N/A	N/A
Case 3/A.3	Reinforced (2 steel drainage pipes + 1 steel pipe)	○	○	○[a]	×/○[b]	○	○
Case 4/A.4	Reinforced (3 steel pipes)	○	×	○[a]	×	○	×
Case 6/A.6	Reinforced (3 drainage pipes)	×	○	×	○	×	○

Note: R = reinforcement function, here pipe made of steel; D = drainage function, here pipes is tubular with holes on the surface; ○ = present; × = not present; N/A = not available, pipes not used; a = with strain gauges to measure axial force and bending moment; b = in numerical analysis for the parametric studies; c = case identification for parametric studies

Table 2 Properties of Edosaki sand

Property	Value
Soil particle density (Mg/m^3)	2.72
Average initial water content of model ground	14.7%
Angle of shearing resistance [Degree of compaction Dc= 80%] (degrees)	29
Cohesion [Dc= 80 %] (kN/m^2)	2.5
Saturated hydraulic conductivity (m/s)	
Foundation	1.5E-6
Levee	4.5E-5
SWCC parameters for van Genuchten model	
Saturated volumetric water content θ_s	0.467
Fitting parameters n	1.674
Fitting parameters α	9.223
Fitting parameters m	0.403
Dry density of foundation (Mg/m^3)	1.72
Dry density of levee (Mg/m^3)	1.45
Modulus of Elasticity (N/m2)	2.55E5

Table 3 Properties of Steel Drainage Pipe

Parameter	Value
Internal diameter (mm)	60
External diameter (mm)	80
Length (m)	6
Embedment length (m)	5.6
Young's Modulus, E (N/m^2)	2.10E+11
Flexural rigidity, EI (Nm^2)	2.89E+5
Poisson's ratio, v	0.3

Table 4 Comparison of the performance of Levee for different Cases

Case	Max settlement (mm)	Max horizontal displacement (mm)	Unsaturated levee cross-section area [a] (m^2)
Case A.1	Levee failure	Levee failure	9.67 (-32.5%) [b]
Case A.3	8.2	14.8	14.33
Case A.4	17.4 (+112.2%) [b]	43.48. (+193.2%) [b]	8.27 (-42.3%) [b]
Case A.6	8.4 (+2.4%) [b]	20.3 (37.2%) [b]	14.33

Note: a = 40 m^2 when the water table is located at the foundation ground surface level, b = percentage change in comparison to Case A.3

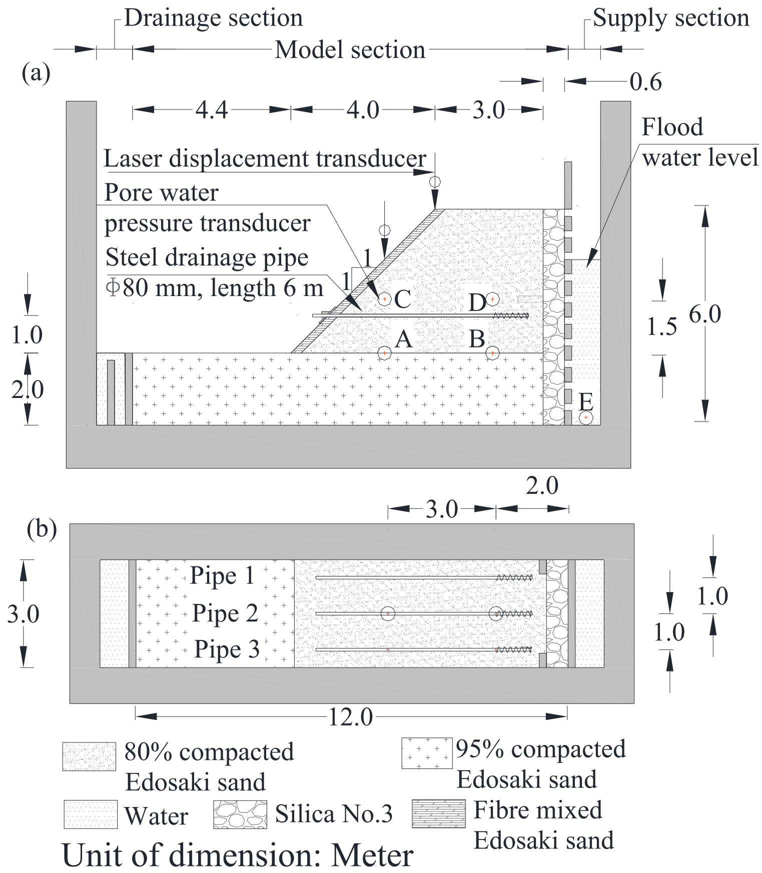

Fig 1 Model Configuration (a) sectional view with geometry and location of sensors (b) plan view (Unit of dimension: meter)

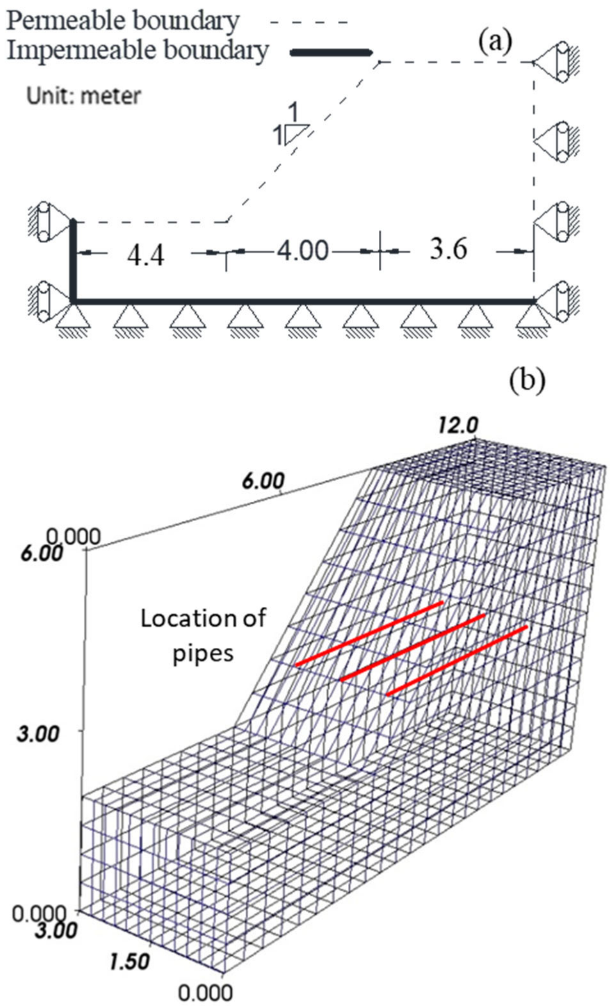

Fig 2 Finite element analysis condition (a) Boundary condition for analysis (b) Mesh for model ground

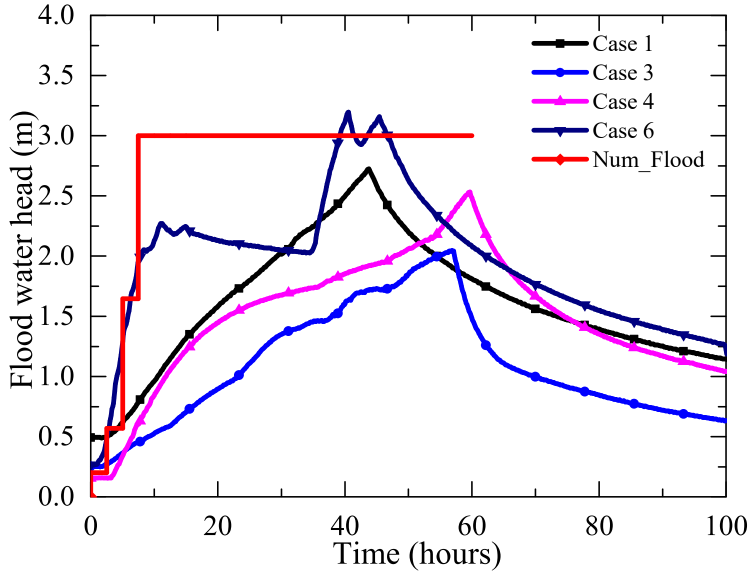

Fig 3 Time histories of supply flood water head

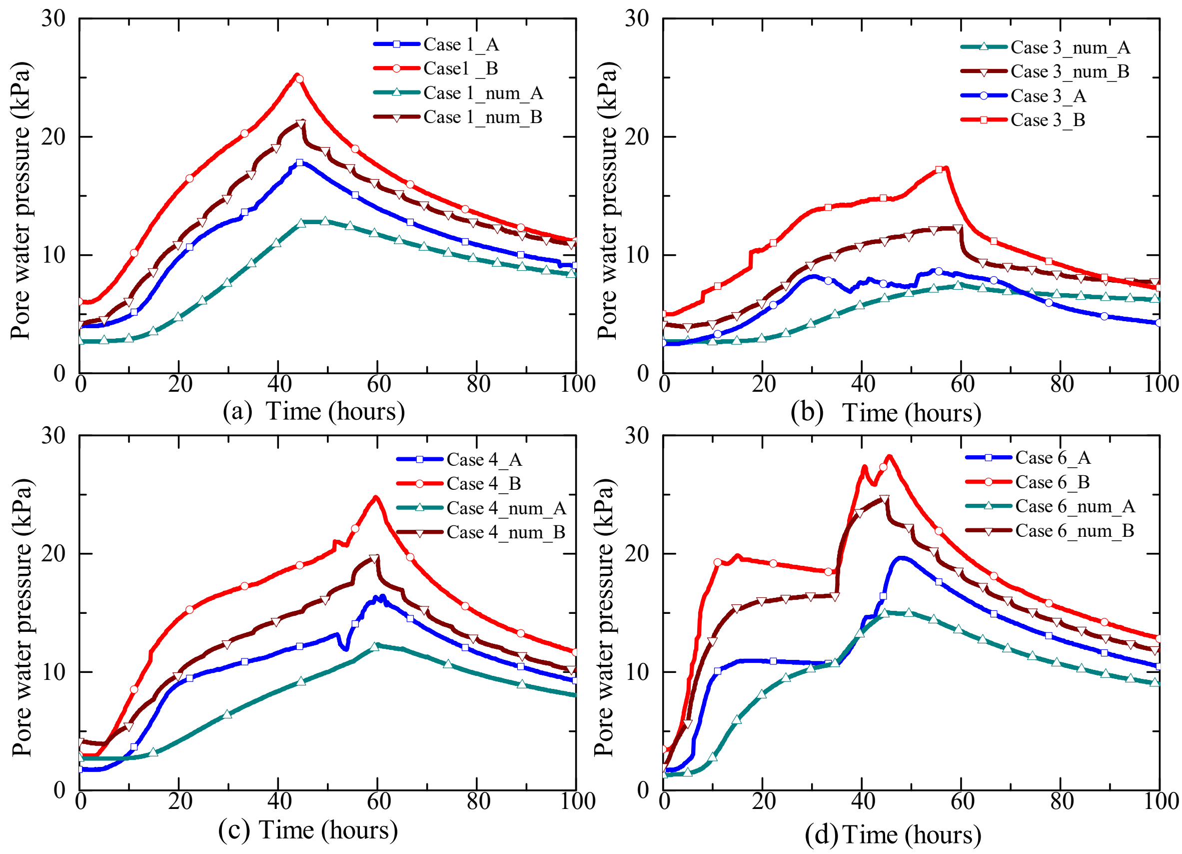

Fig 4 Comparison of the time histories of pore water pressure at locations A (below slope) and B (below crest) for (a) Case 1 (b) Case 3 (c) Case 4 (d) Case 6

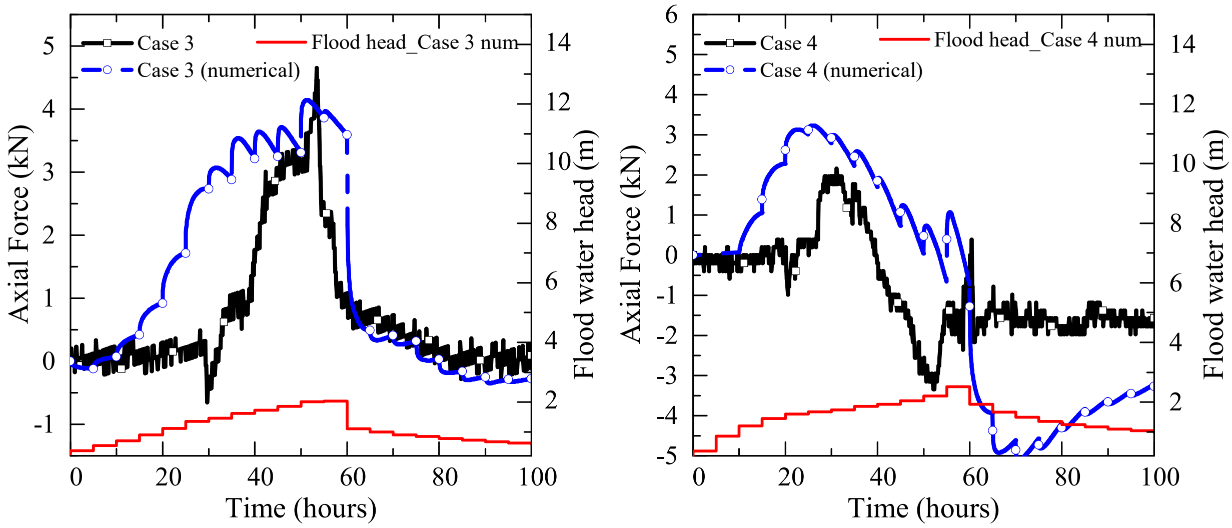

Fig 5 Comparison of the time histories of axial force at 0.4m away from slope surface (a) for Case 2 (b) for Case 3

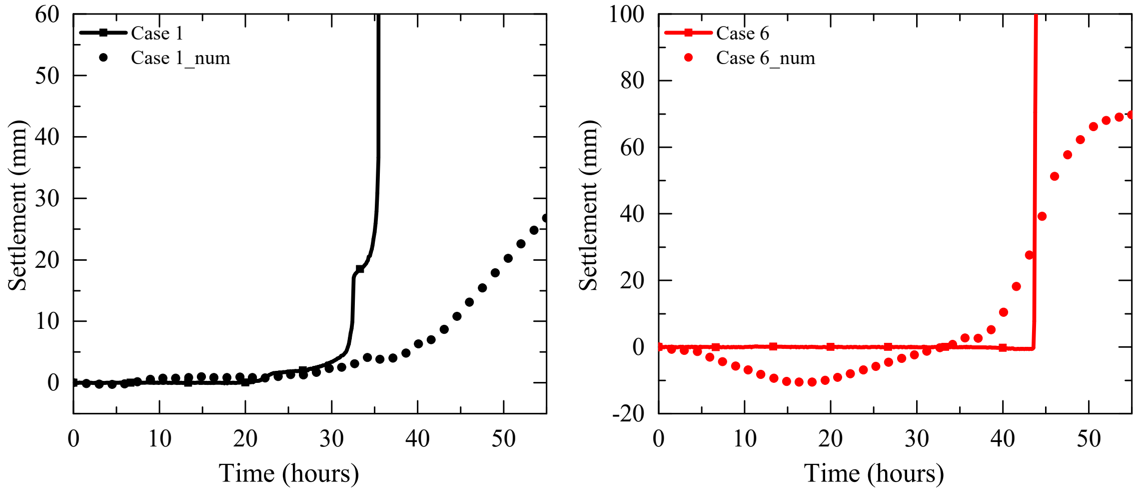

Fig 6 Comparison of the time histories of settlement at location F (a) Case 1 (b) Case 6

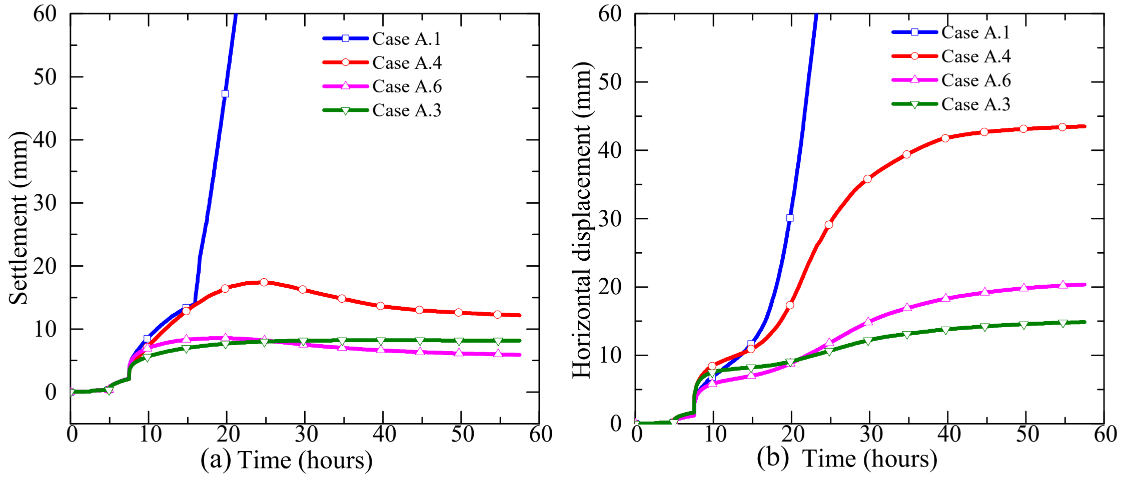

Fig 7 Time histories of displacement for all cases (a) settlement at the shoulder of slope (b) horizontal displacement at the toe of the slope

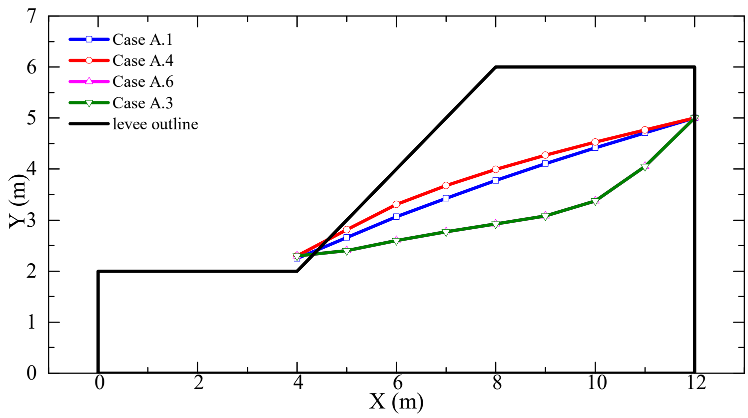

Fig 8 Location of phreatic surfaces in River levee in Cases A.1-A.4 after 40 hours of seepage flow

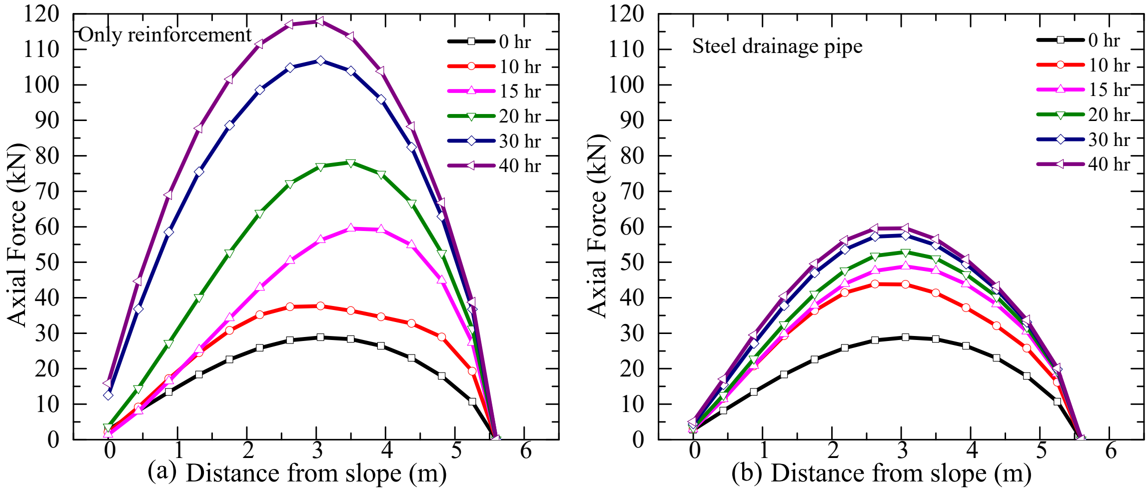

Fig 9 Axial force distribution in the pipe (a) for Case A.4 (only reinforcement) (b) for Case A.3 (steel drainage pipe)

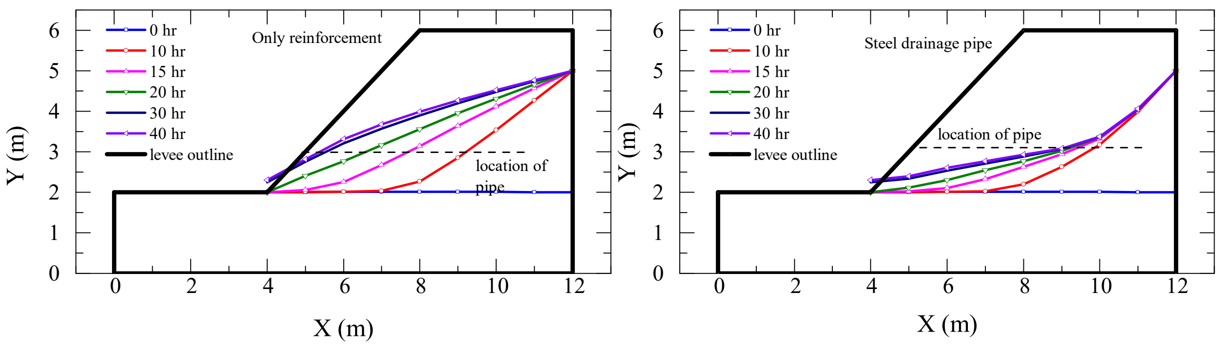

Fig 10 Location of phreatic surfaces (a) for Case A.4 (only reinforcement) (b) for Case A.3 (steel drainage pipe)